

## RESEARCH ARTICLE

# Whole-tree sap flux in *Quercus serrata* trees after three levels of partial sapwood removal to simulate Japanese oak wilt

G. G. T. Chandrathilake<sup>1,2</sup> | Nobuaki Tanaka<sup>3</sup> | Naoto Kamata<sup>4</sup>

<sup>1</sup>Education and Research Center, University of Tokyo Forests, Graduate School of Agricultural and Life Sciences, The University of Tokyo, 1-1-1, Yayoi, Bunkyo-ku, Tokyo, 113-8657, Japan

<sup>2</sup>Department of Forestry and Environmental Sciences, Faculty of Applied Sciences, University of Sri Jayewardenepura, Gangodawila, Nugegoda, Sri Lanka

<sup>3</sup>Ecohydrology Research Institute, University of Tokyo Forests, Graduate School of Agricultural and Life Sciences, The University of Tokyo, Seto-Shi, Aichi, Japan

<sup>4</sup>University of Tokyo Hokkaido Forest, University of Tokyo Forests, Graduate School of Agricultural and Life Sciences, The University of Tokyo, Furano, Hokkaido, Japan

## Correspondence

G.G.T. Chandrathilake, Education and Research Center, University of Tokyo Forests, Graduate School of Agricultural and Life Sciences, The University of Tokyo, 1-1-1, Yayoi, Bunkyo-ku, Tokyo, 113-8657, Japan. Email: thilakawansa@gmail.com

## Funding information

Japan Society for the Promotion of Science.

## Abstract

Plant transpiration plays a key role in the hydrological cycle in forested watersheds. Oak trees infested with Japanese oak wilt may show changes in transpiration even if they are still alive. However, to our knowledge, no study has shown changes in transpiration and its threshold for tree weakening. We hypothesized that whole-tree sap flux would be reduced in surviving oak trunks owing to sapwood dysfunction; however, part of this reduction would be compensated by enhanced sap flux density (*F<sub>d</sub>*) in the remaining functioning sapwood. To test this hypothesis, 25%, 50%, and 75% of sapwood was removed at breast height to simulate xylem dysfunction for nine *Quercus serrata* trees in a warm-temperate secondary forest in Japan. Granier probes were used to measure the *F<sub>d</sub>* of the treated and three control trees before and after the treatment. Even though tested trees were still alive until at least the end of the second growing season, external symptoms of weakening were detected in 75% treated trees. Analysis using a linear mixed model showed that whole-tree sap flux was significantly reduced in all treatments. However, 25% and 50% treated trees showed significant *F<sub>d</sub>* compensation, whereas 75% treated trees showed significantly smaller whole-tree sap flux than the value expected from the treatment. These results suggest that the threshold of tree weakening lies between 50% and 75% of sapwood removal, above which the *F<sub>d</sub>* compensation cannot be attained. Therefore, whole-tree sap flux in infested but surviving trees varies with respect to the intensity of sapwood damage.

## KEYWORDS

ambrosia beetle, ambrosia fungi, Granier method, *Platypus quercivorus*, radial growth, *Raffaelea quercivora*, tree mortality, tree transpiration

## 1 | INTRODUCTION

Incidences of Japanese oak wilt (JOW) have been recorded since the 1930s in Japan, with epidemics being documented since the late 1980s (Kamata, Esaki, Kato, Igeta, & Wada, 2002). Consequently, the mass mortality of trees belonging to the family Fagaceae during the summer months has become a serious problem (Kuroda & Yamada, 1996; Ito & Yamada, 1998). JOW is caused by an Ascomycetes fungus *Raffaelea quercivora* that is vectored by an ambrosia beetle *Platypus quercivorus* (Kubono & Ito, 2002). A male beetle excavates an entrance hole into sapwood and uses a pheromone to attract both male and female beetles (Kamata et al., 2002). Only females have mycangia, in which they carry ambrosia that is a mixture of fungi, yeasts, and bacteria; consequently, infection by *R. quercivora* occurs after females start to construct a gallery in sapwood. *R. quercivora* spreads into the

sapwood from the gallery surface and causes necrosis followed by discoloration. The discolored area spreads to areas surrounding the beetle galleries. Vessels in the necrosis are nonconductive (Kuroda & Yamada, 1996; Kuroda, 2001). Therefore, if many beetles attack the host tree, widespread necrosis stops water conductance, leading to the wilting and discoloration of foliage (Saito, Nakamura, Miura, Mikawa, & Onose, 2001). Ultimately, this phenomenon results in branch dieback or even tree mortality (Kuroda & Yamada, 1996). However, some infested trees do not show even branch dieback (Kamata et al., 2002; Murata et al., 2007; Yamasaki, Ito, & Ando, 2014).

The mass mortality of oak trees reduces canopy cover and tree density, which has a major impact on the landscape, dynamics, and conservation of forests (Hata, Iwai, & Sawada, 2014). The mass mortality of trees may also impact ecosystem services due to changes in the hydrological cycle of forests (Matheny et al., 2014) by altering forest

evapotranspiration (Bonan, 2008). Plant–water relations are an important component of ecohydrology, because plant evapotranspiration is important for the hydrological cycle and influences the water budget in forested watersheds (Wang et al., 2010).

*Quercus serrata* is a deciduous oak, which is a dominant tree species in a secondary forest in warm-temperate region in Japan. It has been reported that more than half of *Q. serrata* survive even after JOW disturbance (Urano, 2000; Saito & Shibata, 2012). The infested but surviving trees may appear externally identical to trees without *P. quercivorus* attacks. However, these trees may be weakened internally owing to blockages of sap flow (Kuroda & Yamada, 1996). *Q. serrata* is a canopy-dominant tree species in secondary forests and may be important in determining watershed-scale canopy transpiration. Therefore, before assessing JOW impact on watershed-scale hydrology, we must investigate changes to the magnitudes of tree transpiration in infested but surviving *Q. serrata* trees.

Several methods have been developed to assess and quantify tree transpiration. Sap flow measurements allow whole-tree sap flux to be estimated and are widely used in measuring tree transpiration (Granier, 1987; Ladekarl, 1998; Oren, Phillips, Ewers, Pataki, & Magonigal, 1999; Wilson, Hanson, Mulholland, Baldocchi, & Wullschlegel, 2001; Wang et al., 2010). Sap transports water and nutrients from the roots to foliage and to living cells in trees (Tyree & Sperry, 1988). The combined effect of differences in water potential among the soil, the plant, and the atmosphere, as well as the capillary action of the xylem, causes sap to flow from the roots to canopy foliage (Tyree & Sperry, 1988; Tyree & Ewers, 1991). Whole-tree sap flux can be obtained from spatially averaged sap flux density over the sapwood cross section of a tree and the hydro-active sapwood area of the tree (Granier, 1987; Gartner & Meinzer, 2005; Ford, Hubbard, Kloeppel, & Vose, 2007). Out of the various methods available to measure sap flux density, Granier sensors (thermal dissipation probe) allow plant water use to be estimated *in situ* at relatively low cost and are easy to use in complex terrains (Ladekarl, 1998; Kume et al., 2009; Wang et al., 2010).

In this study, Granier sensors were used to detect changes to whole-tree sap flux in relation to mechanical sap wood removal, which simulated sapwood dysfunction by the JOW. We hypothesized that whole-tree sap flux would be reduced in infested but surviving oaks

trees, due to partial sapwood dysfunction. However, we further hypothesized that, due to enhanced sap flux density in remaining healthy sapwood, the decline in the whole-tree sap flux would be less than expected from the dysfunctional sapwood area (hereafter termed “compensatory effect”). To test these hypotheses, this study aimed to (a) investigate the relationships between whole-tree sap flux and the percentage of xylem dysfunction; (b) examine whether sap flux density had a compensatory effect in the healthy part of sapwood; and (c) elucidate the threshold percentage of vessel dysfunction for weakening a tree. We also examined compensatory radial growth in treated trees as a possible cause for the compensatory effect of sap flux. Insights gained from the present study would improve knowledge of how *Q. serrata* trees with partially damaged sapwood influence the magnitude of tree transpiration; this information may be a prerequisite to understanding watershed-scale hydrology in forests infested by JOW.

## 2 | MATERIALS AND METHODS

### 2.1 | Study site

The study was conducted in the south creek of the Shirasaka sub-watershed in the Akazu Research Forest (AKRF), Ecohydrology Research Institute (ERI), the University of Tokyo, which is located in northeastern part of Aichi Prefecture, central Japan (137°10'E, 35° 12'N; Figure 1). AKRF is a secondary forest in the warm-temperate zone and is composed of a mixture of deciduous and evergreen broadleaved trees and evergreen conifers. The forest canopy is mainly composed of *Q. serrata*, *Chamaecyparis obtusa*, and *Pinus densiflora*. Mean tree height is approximately 20 m. The average topographical inclination is 25°, while elevation ranges from 330 to 360 m. The mean annual temperature and mean annual precipitation were 12.8°C and 1860 mm, respectively (1985–2014; ERI, 2012). The first appearance of JOW in the AKRF was reported in 2007; the epidemic peaked in 2011 (Sawada, 2012; Sawada, Hirao, & Kamata, 2014), and by 2014, most *Q. serrata* (80%) in the forest had been attacked by *P. quercivorus*. Out of the attacked *Q. serrata*, 35% died, while the remaining 65% of trees survived (Sato, Matsui, & Tanaka, 2016).

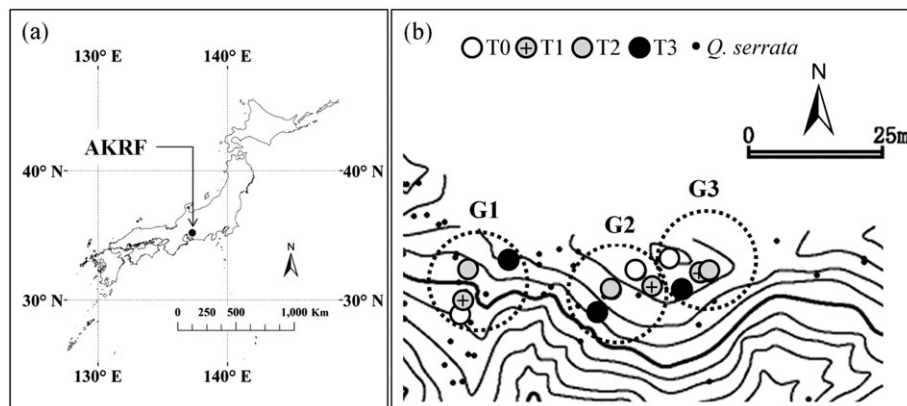


**FIGURE 1** Location of the study site and test trees. (a) Geographical location of Akazu Research Forest (AKRF) in Japan, (b) Topography of the study site in AKRF and the distribution of tested *Quercus serrata* trees within this site. T0 = control; T1, 25% of sapwood removal; T2 = 50% of sapwood removal; T3 = 75% of sapwood removal

## 2.2 | Test trees and sapwood removal

Twelve *Q. serrata* individuals that reached the top canopy layer were selected as test trees (Table 1). The geographical location and history of *P. quercivorus* attacks were considered as the selection criteria. Before starting the experiment, the trunks of the test trees were covered with plastic sheets to prevent natural *P. quercivorus* attacks during the study. The test trees were divided into three groups (G1, G2, and G3) according to the geographical distribution considering the ease of sharing electrical equipment and closer to the electric power source for conducting sap flux measurements (Figure 1). Each group consisted of a control tree (no treatment, T0), a 25% treated tree (with 25% sapwood being removed on the north aspect of the trunk, T1), a 50% treated tree (with 50% of sapwood being on the north-east aspect of the tree, T2), and a 75% treated tree (with 75% of sapwood removal at west-north-east aspect, T3; Figure 2). On July 18, 2014 (day of the year, DOY = 199), sapwood was removed to simulate vessel dysfunction due to *R. quercivorus* vectored by *P. quercivorus*. An approximately 2-cm width of sapwood band, about 4 cm below

reference sensors (see section *Sap flux density measurement*), was removed using a chainsaw and a chisel (Figure 2).

## 2.3 | Sap flux density measurements

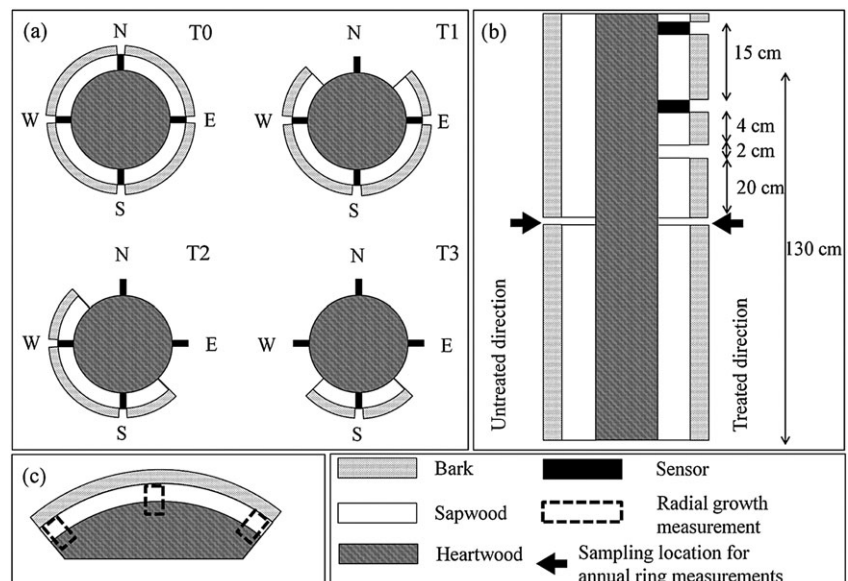
Sap flux densities in four azimuthal directions (north, east, south, and west) of all of the test trees were measured with handmade Granier-type sensors (Granier, 1987) for 130 days from July 15 (DOY = 196) to November 21, 2014 (DOY = 325). Each sensor unit had a continuously heating upper probe and an unheated lower probe (Granier, 1987). A dye injection experiment in a mature *Q. serrata* in the AKRF reported that conductive sapwood thickness varies between 2 and 3 cm at breast height (Sato et al., 2010). Therefore, 20-mm-long probes were used for this study. Several studies suggested that the direct use of the Granier method could underestimate sap flow due to heterogeneous sap flux along the sensor length, especially in ring-porous tree species (Chiu, Tateishi, Komatsu, & Otsuki, 2014; Bush, Hultine, Sperry, & Ehleringer, 2010; Clearwater, Meinzer, Andrade, & Goldstein,

**TABLE 1** Test trees (*Quercus serrata*) for measurement of sap flux density with information on group, treatment, diameter at breast height (DBH), ambrosia beetle attack history, and period of sap flux density data available in the sapwood removal experiment

Group	Treatment	DBH (cm)	Ambrosia beetle attack history (year)							Sap flux density data availability (DOY)
			2007	2008	2009	2010	2011	2012	2013	
G1	T0	25.5	No	No	No	No	Yes	No	No	196–325
	T1	21.0	No	No	No	No	Yes	No	No	196–274
	T2	23.9	No	No	No	No	Yes	No	No	196–325
	T3	30.7	No	No	No	No	Yes	No	No	196–325
G2	T0	31.2	No	No	No	Yes	No	No	No	196–324
	T1	22.6	No	No	No	Yes	No	No	No	196–318
	T2	34.1	No	No	No	Yes	No	No	No	196–325
	T3	22.9	No	No	No	Yes	No	No	No	196–325
G3	T0	24.5	No	No	No	Yes	No	No	No	196–321
	T1	25.5	No	No	No	Yes	No	No	No	196–325
	T2	27.4	No	No	No	Yes	No	No	No	196–323
	T3	26.8	No	No	No	Yes	No	No	No	196–325

T0 = control; T1 = 25% of sapwood removal; T2 = 50% of sapwood removal; T3 = 75% of sapwood removal; DOY = day of the year 2014.

**FIGURE 2** Sapwood removal treatments and Granier probes monitoring sap flux density. (a) Horizontal cross sections, (b) vertical cross section, (c) wood sample used to measure radial growth. T0 = control; T1 = 25% of sapwood removal; T2 = 50% of sapwood removal; T3 = 75% of sapwood removal. N = North; E = East; S = South; W = West



1999). However, we did not calibrate the sensor for *Q. serrata*, because the purpose of this study was to detect temporal changes (before and after the treatment) in observed sap flux.

Each probe had a copper–constantan thermocouple in the middle and was covered with an aluminum tube to obtain homogeneous temperature distribution along the probe length. In each direction at breast height of the trunk, two pieces of bark (1.5 × 1.5 cm in size), 15 cm apart from each other vertically, were removed until the cambium was exposed. Two holes (2.5 mm in diameter and 20 mm in depth) were made on the trunk surface in the center of the two sections of exposed cambium. A probe was inserted into each hole. The upper probe contained a heating coil that was connected to a continuous 0.2-W power supply (Granier, 1987). The unheated lower probe detected the reference temperature. Constantan ends from the two probes were connected together, while the copper ends were connected to a multiplexer (AM16/32B, Campbell Scientific Inc., UT, USA), which was controlled by a data logger (CR1000, Campbell Scientific Inc., UT, USA). After installing the probes, exposed cambium areas were covered with silicone gel to prevent contamination or contact with water. The installed sensors were covered with aluminum foil to prevent exposure to direct sunlight. The temperature difference ( $\Delta T$ ) of the two probes was measured every 30s. The 10-min averages of twenty 30-s measurements were recorded by the data logger.

The canopy of all tested trees was monitored for foliage discoloration, wilted leaves, and branch dieback by observation from the ground. The trees were monitored throughout the period of data collection and between summer and fall of the following year.

## 2.4 | Data screening

Before data analysis,  $\Delta T$  data were screened. Each sensor was checked for a data spike or a noisy pattern in a 10-min  $\Delta T$  time series (Figure 3a). Irregular patterns in  $\Delta T$  may have been caused by an electric surge, because both the data logger and the multiplexer were powered by commercial power. Thus,  $\Delta T$  data that produced a spike or noise were removed from the dataset.

## 2.5 | Sap flux density

Recorded temperature differences were converted to sap flux densities ( $F_d$ ;  $\text{cm}^3 \text{m}^{-2} 10 \text{min}^{-1}$ ) by modifying Granier's empirical equation (Granier, 1985, 1987):

$$F_d = \left( 119 \times 10^{-6} \left( \frac{\Delta T_M - \Delta T}{\Delta T} \right)^{1.23} \right) 600, \quad (1)$$

where  $\Delta T_M$  is the maximum temperature difference, representing the value of  $\Delta T$  when  $F_d$  is assumed to be zero (that usually occurs predawn; Granier, 1985, 1987; Lu, Urban, & Zhao, 2004; Du et al., 2011). In Equation 1, “600” was introduced to convert seconds to 10 min. Determination of  $\Delta T_M$  is crucial for the calculation of  $F_d$  using Equation 1 (Granier, 1985, 1987; Lu et al., 2004). When calculating  $\Delta T_M$ , we considered predawn zero sap flux as well as drift of  $\Delta T_M$  over the period of measurement. Because our  $\Delta T$  time series showed

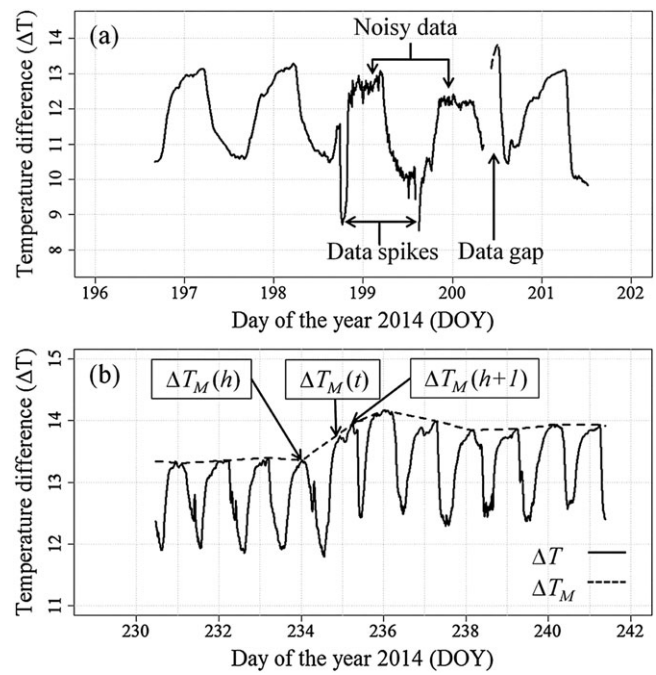


**FIGURE 3** Diurnal variation in temperature difference ( $\Delta T$ ) in 10-min intervals, (a) graph showing noisy data, data gaps, and data spikes for the south direction of the T3 tree (75% of sapwood removed) in study group 2 (G2), (b) determination of maximum temperature differences ( $\Delta T_M$ ) with linear interpolation method for east direction of the T0 tree (control) in study group 1 (G1). “h” represents day 1

considerable daily variations in  $\Delta T_M$  (see an example in Figure 3b),  $\Delta T_M$  was estimated over any given duration of 10 min using the linear interpolation method, based on an assumption that  $F_d$  was zero at the time when the daily maximum  $\Delta T$  was observed. The maximum temperature ( $\Delta T_M$ ) of each sensor on h th date at time t was defined by the following equation (see also Figure 3b):

$$\Delta T_M(t) = \Delta T_M(h) + \left( \frac{\Delta T_M(h+1) - \Delta T_M(h)}{\text{Maxtime}(h+1) - \text{Maxtime}(h)} \right) * (t - \text{Maxtime}(h)), \quad (2)$$

where  $\text{Maxtime}$  is the time when maximum temperature was recorded on a given day. In the 10-min  $F_d$  calculation based on Equation 1, we input  $\Delta T_M(t)$  given by Equation 2 as  $\Delta T_M$ . When  $\Delta T(t) > \Delta T_M(t)$ , we set  $\Delta T(t)$  as  $\Delta T_M(t)$ , because Equation 1 cannot be applied in this case.

After treatment, the  $F_d$  for the treated directions was considered as zero (no sap flow movement). The 10-min  $F_d$  was averaged over the four directions for each individual. For each individual, daily  $F_d$  was calculated from the 10-min averaged  $F_d$  time series. In the data analyses, both 10-min and daily  $F_d$  were separated into two groups: before and after applying the treatment.

## 2.6 | Normalized sap flux density index

To exclude variation in  $F_d$  among individual test trees, both 10-min and daily  $F_d$ s were normalized using each of the averaged  $F_d$  values before treatment for each individual. The normalized indices were used in subsequent data analyses. The normalized sap flux density index ( $nF_d$ )

of  $i$  th tree in  $j$  th group at time/date  $t$  was defined by the following equation:

$$nF_{dij}(t) = \frac{F_{dATij}(t)}{F_{dBT\ mean\ ij}}, \quad (3)$$

where  $F_{dATij}$  is the  $F_d$  of  $i$  th tree in  $j$  th group after treatment and  $F_{dBT\ mean\ ij}$  is the mean  $F_d$  of  $i$  th tree in  $j$  th group before treatment.

## 2.7 | Linear mixed model

To examine how each treatment influenced whole-tree sap flux, a linear mixed model (LMM) was employed, in which either “10-min or daily  $nF_d$ ” was a response variable, “treatment (T0 [control], T1 [25% treated tree], T2 [50% treated tree], and T3 [75% treated tree])” was a fixed effect, and “group” and “date and time” were random effects.

Before investigating whether  $F_d$  had a compensatory effect in the healthy part of sapwood, we calculated an  $F_d$  index (hereafter termed “offset  $F_d$ ”) that would have been observed if the treatment had not been implemented. For each treatment tree, we first derived the proportion of the sum of  $F_d$  in the treated direction(s) in relation to the sum of  $F_d$  in the four directions using directional  $F_d$  data before the treatment ( $p$ ). Then, the offset  $F_d$  indices at the time/date  $t$  for  $i$  th tree in  $j$  th group were calculated by the following equation:

$$osF_{dij}(t) = \frac{nF_{dij}(t)}{p_{ij}}. \quad (4)$$

The calculated offset values ( $osF_d$ ) of treated trees were compared with the  $nF_d$  values of control trees by LMM, in which “10-min or daily  $osF_d$ ” was a response variable, “treatment” was a fixed effect, and “group” and “date and time” were random effects. If the  $osF_d$  of each treatment was positive and significantly greater than 0, it was judged that a compensatory effect of  $F_d$  in the untreated portions of treated trees was present. In contrast, if the  $osF_d$  of each treatment was negative and significantly lower than 0, the treated trees were judged to be weakened.

In order to test the treatment effect on  $F_d$  variation at different intervals, the study period was separated into three seasons—S1 (from July 19 to August 8), S2 (from August 9 to October 1), and S3 (from October 2 to November 21) based on data availability and data gaps of individuals trees (specially G1 T1; Table 1). The three seasons S1, S2, and S3 represent the mid-summer, late-summer, and autumn, respectively. LMMs were used for both 10-min and daily data of S1, S2, S3, and S1–S3 (whole study period).

## 2.8 | Annual growth ring measurement

We hypothesized that compensatory radial growth in treated trees was one of cause for compensatory sap flux in the untreated direction. Two pieces of minor-segment wood samples were collected from each test tree on December 9, 2015, using a hand saw and a chisel (Figure 2c). The samples were taken from the north (treated direction) and the south (untreated direction) directions of a trunk at approximately 20 cm below the position of sapwood removal (Figure 2b).

Radial growth in each year from 2013 to 2015 was determined at three positions for each wood sample by microscopic observation (SZX7, Olympus, Japan; Figure 2c). For both treated and untreated directions, the ratios of radial growth (2014 growth/2013 growth and 2015 growth/2013 growth) were compared between T0 (control) and all other treatments. A linear model (LM) was used, in which the “ratio” was a response variable and the “treatment” was an explanatory variable.

## 3 | RESULTS

Foliage coloration indicated that all individuals of the control and treated trees were still alive at the end of the experimental. Branch die-back was also absent in all test trees during the experiment period up to mid-October 2015. However, twigs with no living leaves and relatively sparse canopy foliage were detected for T3 (75% treated trees).

The LMM results on the effects of “treatment” on  $nF_d$  (Table 2) showed that intercepts (and so the sap flux) of control trees decreased with season. The coefficients of all three treatments were significantly negative in each of the three seasons and for all seasons combined (S1–S3), with one exception, showing that whole-tree sap flux was significantly reduced by sapwood removal. The only exception was T1 (25% treated tree) in S3, where the obtained negative coefficient did not significantly differ from 0 for daily data, but did significantly differ for 10-min data. The absolute values of the coefficients were greatest for T3 (75% treated tree) followed by T2 (50% treated tree), with a greater reduction in whole-tree sap flux occurring as the percentage of sapwood removal increased. The absolute values of the coefficients tended to decrease with season, showing that the reduction in whole-tree sap flux decreased with season.

The LMM results on the compensatory effects (Table 3) showed that the coefficients of T1 (25% treated tree) and T2 (50% treated tree) were all positive and significantly differed from “0,” indicating significant  $F_d$  compensation in the untreated sapwood. The positive coefficient (and so compensatory effect) of T2 (50% treated tree) was consistently greater than that of T1 (25% treated tree). In the 10-min data, the coefficients of T3 (75% treated tree) were negative and significantly differed from “0” in S1 and S2, indicating that the reduction in whole-tree sap flux was greater than that expected from sapwood removal. The coefficient of T3 (75% treated tree) in S3 was positive, but not significantly different from “0,” indicating no  $F_d$  compensation in the untreated sapwood. The coefficients of T3 (75% treated tree) were all negative without any significant difference to “0” for the daily data. The coefficient values of T2 (50% treated tree) and T3 (75% treated tree) in both the 10-min and daily timescales tended to increase from S1 to S3, indicating that the compensatory effect increased with season. The coefficient value of T1 (25% treated tree) in both the 10-min and daily timescale was greatest in S3, followed by S1.

The relationship between whole-tree sap flux and percentage of sapwood removal in treated and control trees is presented in Figure 4. Using the posttreatment daily  $nF_d$  dataset (23 days where  $nF_d$  are available for all examined individuals), we calculated the total  $nF_d$  for each individual during this period, and then the calculated totals

**TABLE 2** Results of the linear mixed models for analyzing the effects of sapwood removal over three seasons and for all seasons combined. Control trees were used as base models. (a) 10-min normalized sap flux density data; (b) daily normalized sap flux density data

(a)				
Season (day of the year 2014)	Treatment	Estimate	t value	pr(> t )
S1 (200–220)	Intercept	0.81	12.06	<.01**
	T1	-0.16	-34.19	<.01**
	T2	-0.34	-74.98	<.01**
	T3	-0.62	-136.03	<.01**
S2 (201–274)	Intercept	0.61	10.57	<.01**
	T1	-0.12	-43.89	<.01**
	T2	-0.20	-73.76	<.01**
	T3	-0.47	-177.60	<.01**
S3 (275–325)	Intercept	0.42	12.56	<.01**
	T1	-0.03	-8.69	<.01**
	T2	-0.07	-24.36	<.01**
	T3	-0.31	-111.60	<.01**
S1–S3 (200–325)	Intercept	0.57	12.93	<.01**
	T1	-0.09	-46.71	<.01**
	T2	-0.17	-96.11	<.01**
	T3	-0.44	-240.72	<.01**
(b)				
Season (day of the year 2014)	Treatment	Estimate	t value	pr(> t )
S1 (200–220)	Intercept	0.82	10.82	<.01**
	T1	-0.16	-6.43	<.01**
	T2	-0.35	-14.35	<.01**
	T3	-0.64	-25.89	<.01**
S2 (201–274)	Intercept	0.61	10.42	<.01**
	T1	-0.11	-6.13	<.01**
	T2	-0.19	-10.86	<.01**
	T3	-0.47	-26.54	<.01**
S3 (275–325)	Intercept	0.44	12.72	<.01**
	T1	-0.03	-1.58	.114
	T2	-0.07	-3.97	<.01**
	T3	-0.32	-17.97	<.01**
S1–S3 (200–325)	Intercept	0.59	13.24	<.01**
	T1	-0.09	-7.01	<.01**
	T2	-0.18	-14.01	<.01**
	T3	-0.45	-36.50	<.01**

T1 = 25% of sapwood removal; T2 = 50% of sapwood removal; T3 = 75% of sapwood removal.

\*\* .01 statistical significance.

\* .05 statistical significance.

were averaged for each treatment type (i.e., T0 [control] to T3 [75% treated tree]). Whole-tree sap flux decreased gradually as the percentage of sapwood removal increased (Figure 4). In contrast, for T1 (25% treated tree) and T2 (50% treated tree),  $F_d$  compensation was detected, which was shown by the greater incidence of whole-tree sap flux than the expected (Figure 4). Compensatory effect was greater in T2 (50% treated tree) than T1 (25% treated tree; Figure 4). In contrast, observed whole-tree sap flux in T3 did not differ from the expected value (Figure 4).

The trunks of trees grew radially in both treated (south) and untreated (north) directions, even after treatment, because the ratio of radial growth was greater than 0 (Figure 5). However, the treatment depressed the radial growth of the treated direction, because the ratios of T1 (25% treated tree) to T3 (75% treated tree) were smaller than those of T0 (control; Figure 5a,b). In contrast, in both years, the ratio

**TABLE 3** Results of the linear mixed models used to analyze  $-F_d$  compensation (or compensatory effects on whole-tree sap flux) following sapwood removal over three seasons and for all seasons combined. Control trees were used as base models (a) 10-min normalized sap flux density data; (b) daily normalized sap flux density data

(a)				
Season (day of the year 2014)	Treatment	Estimate	t value	pr(> t )
S1 (200–220)	Intercept	0.81	5.45	.03 <sup>†</sup>
	T1	0.05	10.70	<.01**
	Intercept	0.82	5.68	.03 <sup>†</sup>
	T2	0.16	31.31	<.01**
S2 (201–274)	Intercept	0.79	11.77	<.01**
	T3	-0.02	-5.82	<.01**
	Intercept	0.61	4.26	.04 <sup>†</sup>
	T1	0.02	5.79	<.01**
S3 (275–325)	Intercept	0.59	4.42	.04 <sup>†</sup>
	T2	0.27	80.26	<.01**
	Intercept	0.60	29.21	<.01**
	T3	-0.02	-6.91	<.01**
S1–S3 (200–325)	Intercept	0.56	4.28	.02 <sup>†</sup>
	T1	0.05	24.66	<.01**
	Intercept	0.55	5.30	.03 <sup>†</sup>
	T2	0.28	117.60	<.01**
S3 (275–325)	Intercept	0.56	35.23	<.01**
	T3	-0.01	-4.59	<.01**
	Intercept	0.38	3.07	.09
	T1	0.08	20.59	<.01**
S1–S3 (200–325)	Intercept	0.38	5.69	.03 <sup>†</sup>
	T2	0.33	83.59	<.01**
	Intercept	0.43	24.08	<.01**
	T3	0.01	1.78	.07
S1 (200–220)	Intercept	0.81	4.98	.03 <sup>†</sup>
	T1	0.05	2.48	.02 <sup>†</sup>
	Intercept	0.82	5.29	.03 <sup>†</sup>
	T2	0.16	5.58	<.01**
S2 (201–274)	Intercept	0.80	9.37	<.01**
	T3	-0.04	-1.09	.28
	Intercept	0.62	4.21	.05 <sup>†</sup>
	T1	0.02	1.12	.27
S3 (275–325)	Intercept	0.59	4.16	.04 <sup>†</sup>
	T2	0.28	3.61	<.01**
	Intercept	0.61	16.58	<.01**
	T3	-0.03	-1.07	.28
S1–S3 (200–325)	Intercept	0.57	4.30	.05 <sup>†</sup>
	T1	0.05	4.55	<.01**
	Intercept	0.56	5.18	.03 <sup>†</sup>
	T2	0.28	18.94	<.01**
S3 (275–325)	Intercept	0.58	20.17	<.01**
	T3	-0.03	-1.33	.18
	Intercept	0.40	5.66	.02 <sup>†</sup>
	T2	0.33	17.17	<.01**
S1–S3 (200–325)	Intercept	0.45	13.43	<.01**
	T3	-0.01	-0.40	.68
	Intercept	0.45	13.43	<.01**
	T3	-0.01	-0.40	.68

T1 = 25% of sapwood removal; T2 = 50% of sapwood removal; T3 = 75% of sapwood removal.

\*\* .01 statistical significance.

\* .05 statistical significance.

for the untreated direction was significantly greater in T1 (25% treated tree) than in T0 (control; LM,  $p < .01$ ; Figure 5c,d), supporting

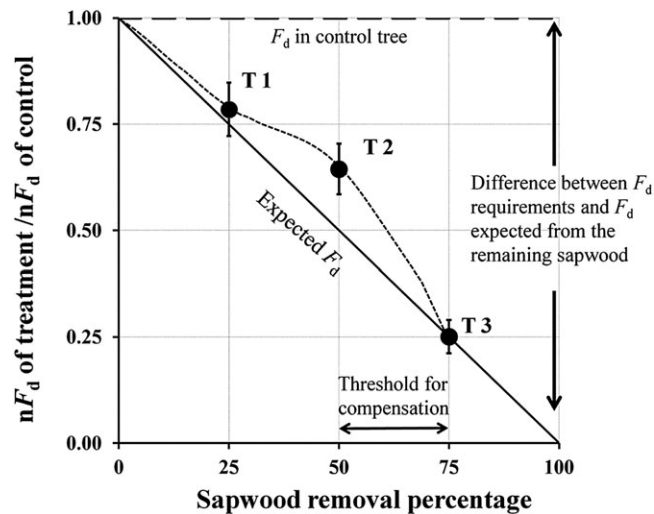


**FIGURE 4** Relationship between whole-tree sap flux and the different sapwood removal percentage. Solid circles represent the ratios of averaged normalized sap flux density ( $nFd$ ) for T1, T2, and T3, respectively, in relation to the averaged  $nFd$  for T0; thus, showing the observed whole-tree sap flux in treated trees compared with control trees. Error bars represent standard deviation of sap flux density. T1, T2, and T3 were combined by a hand-drawn curve (dashed curve) to show the trend. Stem sap flow of woody plants was estimated from the product of multiplying sap flux density by the cross-sectional sapwood area of active xylem or sapwood (Köstner et al., 1992). Therefore, for treated trees, posttreatment sap flux was expected to reduce in proportion to the amount of removed sapwood area (a solid line), assuming no substantial circumferential variation in sap flux density ( $F_d$ ). Broken line represents the whole-tree sap flux of the control tree. Up/down arrows represent differences between the sap flux requirements of the control tree and sap flux expected from the remaining sapwood. A threshold for compensation is shown by the range of the left to right arrow. T0 = control; T1 = 25% of sapwood removal; T2 = 50% of sapwood removal; T3 = 75% of sapwood removal

compensatory radial growth in the treatment group. For T2 (50% treated tree) and T3 (75% treated tree), no significant difference from T0 (control) was found in the ratio for the untreated direction (LM,  $p > .05$ ; Figure 5c,d).

## 4 | DISCUSSION

The LMM analysis of treatment effect and compensatory effect indicated that the coefficients of the treatments differed significantly from 0, which means that tree-to-tree  $F_d$  variation was low compared with the  $F_d$  variation due to the treatment. Therefore, three replicates ( $n = 3$ ) per treatment type were sufficient to ensure that the final results were accurate.

In trees, water (sap flow) transport from roots to leaves relies on negative pressures established in continuous water columns in xylem conduits as described in cohesive tension theory. On the other hand, sap flow movement of a tree largely depends on total conductive sapwood area (Granier, 1985; Granier, 1987; Granier et al., 1994; Wullschlegel & Norby, 2001; Gartner & Meinzer, 2005; Ford et al., 2007; Gebauer, Horna, & Lesuschner, 2008). Therefore, sap wood

removal treatment caused greater reduction of hydraulic conductivity through reduction in the number of conduits (xylem) supporting the same canopy foliage compared with the before-treatment condition. Moreover, the treatment also reduced water storage capacity that determines the ability of trees to survive water stress conditions (Tyree & Ewers, 1991). Loss of water storage capacity and decreased hydraulic conductance of xylem may lead to a reduction in the water potential in leaves, which might impair plant physiological activities and possibly lead to the eventual death of the plant (Nardini, Lo, & Salleo, 2011). Therefore, in this experiment it was expected that loss in xylem hydraulic conductivity would be proportional to reduced sapwood area. However, our results showed that loss of hydraulic conductivity in treated trees was not proportional to the sapwood removal percentages.

The “pipe model theory of plant form” (Shinozaki, Yoda, Hozumi, & Kira, 1964) regards a plant as an assemblage of “unit pipes,” in which each pipe supports a unit of leaves in the canopy. This theory predicts sectoral canopy wilting and/or branch dieback even if the spiral ascent of sap that has been reported for other species belonging to the genus *Quercus* (Kozłowski & Winget, 1963; Waisel, Lipshitz, & Kuller, 1972) occurs in *Q. serrata*. However, neither canopy wilting nor branch dieback were observed in treated trees. Yet, continuous radial growth was identified at the position below the treatment site in the year following the treatment (Figure 5b). This result provides evidence for the horizontal movement of carbohydrates. Previous studies on sap flow analysis using deuterium oxide ( $D_2O$ ) tracing techniques have reported the axial and radial transport of water within a tree stem (James et al., 2003). The radial movement of sap in the stem is significant with intervessel pits between early wood and late wood vessels (Kitin, Fujii, Abe, & Funada, 2004). Therefore, horizontal water movement in the stem may cause foliage to survive in the treated directions.

However,  $F_d$  compensation occurred in the remaining sapwood of treated trees, making up for reduced sap flow by sapwood removal (Table 3, Figure 4). Given that  $F_d$  compensation increased with the ratio of removed sapwood to remaining sapwood, the ratio would be 0.33 (=25/75), 1 (=50/50), and 3 (=75/25) in T1 (25% treated tree), T2 (50% treated tree), and T3 (75% treated tree), respectively. These expected ratios indicated that compensation was greatest in T3 (75% treated tree) followed by T2 (50% treated tree). However, whole-tree sap flux in T3 (75% treated tree) was smaller than expected, probably because the trees in T3 (75% treated tree) were highly stressed by a greater proportion of sapwood removal and had begun to weaken. Twigs without leaves and sparse canopy were observed in T3 (75% treated tree) the following year (2015), representing symptoms of weakening. We proposed a threshold for compensation and weakening between 50% and 75% of sapwood dysfunction (Figure 4).

In T1 (25% treated tree) and T2 (50% treated tree), the  $F_d$  compensation was not enough to recover reduced  $F_d$ , which was proportional to sapwood removal. However, signs of weakening and branch dieback were not detected in T1 (25% treated tree) and T2 (50% treated tree). Sap flux may have been enhanced in the remaining sapwood after treatment. Sapwood removal reduces the total number of vessels in the stem without decreasing the amount of canopy foliage and water absorbent area (root hairs), which may increase the velocity of sap flow. Speeding up sap flow movement in the remaining sapwood could

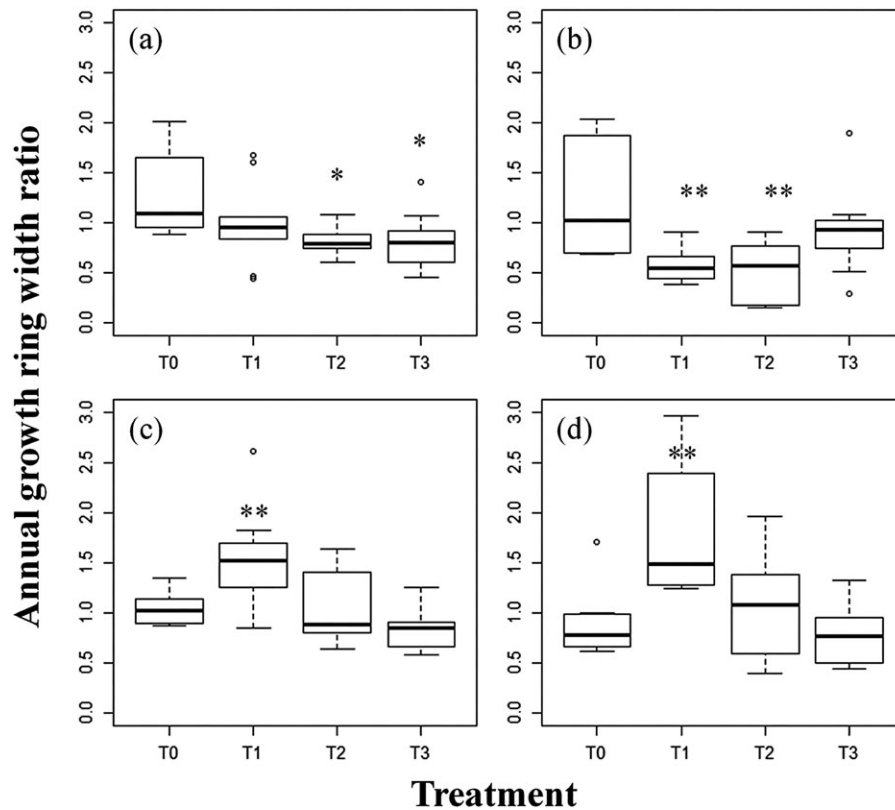


**FIGURE 5** Trunk radial growth after sapwood removal for treated (north) and untreated (south) directions. Ratios for radial growth in 2013 are shown for 2014 and 2015. (a) North, 2014; (b) North, 2015; (c) South, 2014; (d) South 2015. Top bar, maximum; lower bar, minimum; top of a box, third quartile; bottom of the box, first quartile; middle thick bar in the box, median. To examine the influence of treatment type on the width of annual growth rings, a linear model was used, in which “growth ring width ratio” was a response variable, “treatment (T0, T1, T2, and T3)” was an explanatory variable;  $p$ -value  $<.05$  is considered significant ( $*p < .05$ ;  $**p < .01$ ). T0 = control; T1 = 25% of sapwood removal; T2 = 50% of sapwood removal; T3 = 75% of sapwood removal

be a major mechanism of the compensatory effect detected in this experiment.

After applying heat treatment to *Pinus halepensis* stems in early spring, the opposite side of the trunk to the treated direction achieved higher radial growth than the mean radial growth at the breast height level of the tree (Ducrey, Duhoux, Huc, & Rigolot, 1996). The recovery of hydraulic conductivity in ring-porous *Fraxinus excelsior* after winter embolism has also been reported to be entirely dependent on the production of new early wood conduits (Hacke & Sauter, 1996). The compensatory radial growth observed in the untreated direction of T1 (25% treated tree; Figure 5c) may also cause compensatory sap flux in the treatment group. However, no significant compensatory radial growth was found in T2 (50% treated tree; Figure 5c), despite the compensatory sap flux observed in the treatment group (Figure 4). Therefore, compensatory radial growth was not the only cause of compensatory sap flux. However, the gradual recovery of whole-tree sap flux in treated trees with seasonal progression (Table 3) provides indirect evidence for compensatory radial growth, because a certain amount of time is required for radial growth and vessel formation to occur following treatment.

The annual rings of ring-porous wood consist of early wood vessels with large diameters and late wood vessels with narrow diameters (Bush et al., 2010). Consequently, water conductance is mostly restricted to the outermost annual growth ring (Granier et al., 1994; Bush et al., 2010; Sato et al., 2010; Chiu et al., 2014; Taneda & Sperry, 2008). However, there is

considerable sap flow movement in the old inner xylem, as shown by sap flux studies of ring-porous ash (*F. excelsior*) (Gebauer et al., 2008), and *Quercus petraea* and *Quercus robur* (Granier et al., 1994); a similar conclusion was reached in vessel refilling studies in *Quercus gambelii* (Taneda & Sperry, 2008) and in a dye injection experiment in *Q. serrata* (Sato et al., 2010). The ability of sap flow movement in the inner rings increases significantly, after decreasing in the outermost rings, so that the sap flow rate remained unchanged (Granier et al., 1994). Recent studies on xylem physiology have suggested three important mechanisms for the generation of the positive pressure required for refilling embolized conduits: (a) an increase in the osmotic pressure of the remaining sap layer at the inner conduit wall with solutes—this could lower the osmotic potential in the embolized conduits and cause them to refill; (b) reversal of osmotic pressure by starch hydrolysis in adjacent tissues and development of a kind of pumping mechanism to pressurize embolized vessels and refill them under positive pressure; (c) an increase phloem pressure by hormone mediation might drive water transport to the embolized conduit (Taneda & Sperry, 2008; Salleo, Trifilò, & Esposito, 2009; Nardini et al., 2011; Christman, Sperry, & Smith, 2012). To compensate for the loss of hydraulic conductance in treated *Q. serrata* trees, sap flow in the inner conductive xylem might be enhanced by the above-described positive pressure refilling mechanisms. Therefore enhanced sap flow in the inner xylem (but within sensor reach) might also have contributed to the compensatory effect detected in this experiment.

Variation in the symptoms shown by the canopy foliage among the treated trees in this study may serve as a rough indicator of the impact of JOW on watershed-scale canopy transpiration. If most infested oaks in a stand are free from the external symptoms of JOW, as shown for T1 (25% treated tree) and T2 (50% treated tree), the impact of JOW on watershed-scale canopy transpiration is expected to be small. This is because the reduction of whole-tree sap flux in infested oaks is mitigated by the compensatory effect. In contrast, if most infested trees exhibit canopy discoloration or twig dieback, as shown for T3 trees, watershed-scale canopy transpiration is significantly reduced. This is because sapwood damage of infested oaks is beyond the threshold for the detected compensatory effect (Figure 4). Of course, because an oak with a permanently wilted canopy stops tree transpiration, the mortality rate represents another important indicator of the impact of JOW on canopy transpiration at the watershed scale.

## 5 | CONCLUSIONS

We examined variation in the whole-tree sap flux of *Q. serrata* stems after three levels of sapwood removal, which simulated vessel dysfunction due to JOW. Our results showed that the three levels of treatments caused significant reduction in whole-tree sap flux. Twenty-five percent and 50% treated trees showed significant sap flux compensation, whereas 75% treated trees showed no compensatory effects at all. The threshold for showing compensation ranged between 50% and 75% of vessel dysfunction, but was probably closer to 75%, because the observed whole-tree sap flux of T3 (75% treated tree) did not differ to the sap flux expected from the remaining sapwood. To our knowledge, this study is the first to identify the whole-tree sap flux compensatory effect in treated but surviving trees. Compensatory radial growth in the untreated direction was detected in 25% treated trees, which caused the compensation in whole-tree sap flux. Increased sap flow ascent in the inner xylem may also contribute to this phenomenon. The physiological mechanisms supporting the compensatory effect could not be fully assessed; however, the present study reveals how infested, but surviving, *Q. serrata* trees control the magnitude of whole-tree transpiration. This information will be useful in better understanding watershed-scale hydrology in forests disturbed by JOW.

## ACKNOWLEDGMENTS

This work was supported by Grants-in-aid for Scientific Research (23255011) by Japan Society for the Promotion of Science. We express our sincere thanks to staff in Ecohydrology Research Institute, University of Tokyo, for their assistance with fieldwork. We also thank all members in Education and Research Center and the University Tokyo Tanashi Forest, The University Tokyo Forest, Graduate School of Agricultural and Life Sciences, The University of Tokyo.

## REFERENCES

Bonan, G. B. (2008). Forests and climate change: Forcings, feedbacks, and the climate benefits of forests. *Science*, 320, 1444–1449.

- Bush, S. E., Hultine, K. R., Sperry, J. S., & Ehleringer, J. R. (2010). Calibration of thermal dissipation sap flow probes for ring- and diffuse-porous trees. *Tree Physiology*, 30, 1545–1554. doi:10.1093/treephys/tpq096
- Chiu, C. W., Tateishi, M., Komatsu, H., & Otsuki, K. (2014). Comparison of transpiration for *Quercus serrata* estimated based on the sap-flux method and measured based on the cutting-tree experiment. *Bulletin of Kyushu University Forests*, 95, 1–4.
- Christman, M. A., Sperry, J. S., & Smith, D. D. (2012). Rare pits, large vessels and extreme vulnerability to cavitation in a ring-porous tree species. *New Phytologist*, 193, 713–720. doi:10.1111/j.1469-8137.2011.03984.x
- Clearwater, M. J., Meinzer, F. C., Andrade, J. L., Goldstein, G., & Holbrook, N. M. (1999). Potential errors in measurement of nonuniform sap flow using heat dissipation probes. *Tree Physiology*, 19, 681–687.
- Du, S., Wang, Y.-L., Kume, T., Zhang, O. K., Yamanaka, N., & Liu, G.-B. (2011). Sapflow characteristics and climatic responses in three forest species in the semiarid Loess Plateau region of China. *Agricultural and Forest Meteorology*, 151, 1–10. doi:10.1016/j.agrformet.2010.08.011
- Ducrey, M., Duhoux, F., Huc, R., & Rigolot, E. (1996). The ecophysiological and growth responses of Aleppo pine (*Pinus halepensis*) to controlled heating applied to the base of the trunk. *Canadian Journal of Forest Research*, 26, 1366–1374.
- Ecohydrology Research Institute (ERI) (2012). The 5th education and research plan of Ecohydrology Research Institute, the University of Tokyo Forests 2011–2020. *Miscellaneous Information, the University of Tokyo Forests*, 51, 305–396.
- Ford, C. R., Hubbard, R. M., Kloeppel, B. D., & Vose, J. M. (2007). A comparison of sap flux-based evapotranspiration estimates with catchment-scale water balance. *Agricultural and Forest Meteorology*, 145, 176–185. doi:10.1016/j.agrformet.2007.04.010
- Gartner, B. L., & Meinzer, F. C. (2005). Structure–function relationships in sapwood water transport and storage. In N. M. Holbrook, & M. A. Zwieniecki (Eds.), *Vascular transport in plants*. (pp. 307–331) San Diego, CA, USA: Elsevier Academic Press.
- Gebauer, T., Horna, V., & Lesuschner, C. (2008). Variability in radial sap flux density patterns and sapwood area among seven co-occurring temperate broad-leaved tree species. *Tree Physiology*, 28, 1821–1830.
- Granier, A. (1985). Une nouvelle méthode pour la mesure du flux desève brute dans le tronc des arbres. *Annales des Sciences Forestières*, 42, 193–200 (in French with English summary).
- Granier, A. (1987). Evaluation of transpiration in a Douglas-fir stand by means of sap flow measurements. *Tree Physiology*, 3, 309–320.
- Granier, A., Anfodillo, T., Sabatti, M., Cochard, H., Dreyer, E., Tomasi, M., ... Breda, N. (1994). Axial and radial water flow in the trunks of oak trees: A quantitative and qualitative analysis. *Tree Physiology*, 14, 1383–1396.
- Hacke, U., & Sauter, J. J. (1996). Xylem dysfunction during winter and recovery hydraulic conductivity in diffuse-porous and ring-porous trees. *Oecologia*, 105, 435–439. doi:10.1007/BF00330005
- Hata, K., Iwai, N., & Sawada, H. (2014). Attack by *Platypus quercivorus* enhances diameter growth of surviving *Quercus serrata*. *Forest Science*, 60, 1024–1028. doi:10.5849/forsci.13-118
- Ito, S., & Yamada, T. (1998). Distribution and spread of mass mortality of oak trees. *Japanese Forest Society*, 80, 229–232 (in Japanese).
- James, S. A., Meinzer, F. C., Goldstein, G., Woodruff, D., Jones, T., Restom, T., ... Campanello, P. (2003). Axial and radial water transport and internal water storage in tropical forest canopy trees. *Oecologia*, 134, 37–45. doi:10.1007/s00442-002-1080-8
- Kamata, N., Esaki, K., Kato, K., Igeta, Y., & Wada, K. (2002). Potential impact of global warming on deciduous oak dieback caused by ambrosia fungus *Raffaella* sp. carried by ambrosia beetle *Platypus quercivorus* (Coleoptera: Platypodidae) in Japan. *Bulletin of Entomological Research*, 92, 119–126. doi:10.1079/BER2002158
- Kitin, P. B., Fujii, T., Abe, H., & Funada, R. (2004). Anatomy of the vessel network within and between tree rings of *Fraxinus lanuginosa* (Oleaceae). *American Journal of Botany*, 91, 779–788.

- Köstner, B. M. M., Schulze, E. D., Kelliher, F. M., Hollinger, D. Y., Byers, J. N., Hunt, J. E., ... Weir, P. L. (1992). Transpiration and canopy conductance in a pristine broad-leaved forest of *Nothofagus*: An analysis of xylem sap flow and eddy correlation measurements. *Oecologia*, *91*, 350–359.
- Kozłowski, T. T., & Winget, C. H. (1963). Patterns of water movement in forest trees. *Botanical Gazette*, *124*, 301–311.
- Kubono, T., & Ito, S.-I. (2002). *Raffaella quercivora* sp. nov. associated with mass mortality of Japanese oak, and the ambrosia beetle (*Platypus quercivorus*). *Mycoscience*, *43*, 255–260.
- Kume, T., Tsuruta, K., Komatsu, H., Kumagai, T., Higashi, N., Shinohara, Y., & Otsuki, K. (2009). Effects of sample size on sap flux-based stand-scale transpiration estimates. *Tree Physiology*, *30*, 129–138. doi:10.1093/treephys/tp0074
- Kuroda, K. (2001). Responses of *Quercus* sapwood to infection with the pathogenic fungus of a new wilt disease vectored by the ambrosia beetle *Platypus quercivorus*. *Japan Wood Research Society*, *47*, 425–429.
- Kuroda, K., & Yamada, T. (1996). Discoloration of sapwood and blockage of xylem sap ascent in the trunks of wilting *Quercus* spp. following attack by *Platypus quercivorus*. *Journal of the Japanese Forest Society*, *78*, 84–88 (in Japanese with English abstract).
- Ladekarl, U. (1998). Estimation of the components of soil water balance in a Danish oak stand from measurements of soil moisture using TDR. *Forest Ecology and Management*, *104*, 227–238.
- Lu, P., Urban, L., & Zhao, P. (2004). Granier's thermal dissipation probe (TDP) method for measuring sap flow in trees: Theory and practice. *Acta Botanica Sinica*, *46*, 631–646.
- Matheny, A. M., Bohrer, G., Vogel, C. S., Morin, T. H., He, L., Frasson, R. P. M., ... Curtis, P. S. (2014). Species-specific transpiration responses to intermediate disturbance in a northern hardwood forest. *Journal of Geophysical Research: Biogeosciences*, *119*, 1–20. doi:10.1002/2014JG002804
- Murata, M., Yamada, T., Matsuda, Y., & Ito, S. (2007). Discoloured and non-conductive sapwood among six *Fagaceae* species inoculated with *Raffaella quercivora*. *Forest Pathology*, *37*, 73–79.
- Nardini, A., Lo, G. M. A., & Salleo, S. (2011). Refilling embolized xylem conduits: Is it a matter of phloem unloading? *Plant Science*, *180*, 604–611. doi:10.1016/j.plantsci.2010.12.011
- Oren, R., Phillips, N., Ewers, B. E., Pataki, D. E., & Mezonigal, J. P. (1999). Sap-flux-scaled transpiration responses to light, vapor pressure deficit, and leaf area reduction in a flooded *Taxodium distichum* forest. *Tree Physiology*, *19*, 337–347.
- Saito, S., & Shibata, M. (2012). The forest structure and tree death of forest stands damaged by Japanese oak wilt in Yamagata prefecture. *Journal of Japanese Forestry Society*, *94*, 223–228 (in Japanese with English abstract).
- Saito, S., Nakamura, H., Miura, N., Mikawa, K., & Onose, K. (2001). Process of mass oak mortality and the relation to *Platypus quercivorus* and its specific fungus. *Japanese Forest Society*, *83*, 58–61 (in Japanese with English summary).
- Salleo, S., Trifilò, P., & Esposito, S. (2009). Starch-to-sugar conversion in wood parenchyma of field-growing *Laurus nobilis* plants: A component of the signal pathway for embolism repair? *Functional Plant Biology*, *36*, 815–825.
- Sato, T., Matsui, M., Tanaka, N., & Kuraji, K. (2016). Temporal variation of infestation by *Platypus quercivorus* (Murayama) in a warm-temperate secondary forest stand in Tokai District. *Chubu Forestry Research*, *64*, 47–50 (in Japanese).
- Sato, T., Tanaka, N., Inoue, M., Sawada, H., Watanabe, S., & Suzuki, M. (2010). Report on an experiment of dye injection into xylem sap of a *Quercus serrata* tree in University Forest in Aichi. *Miscellaneous Information, the University of Tokyo Forests*, *49*, 29–41 (in Japanese with English abstract).
- Sawada, H. (2012). Initial stage infestation of *Platypus quercivorus* in the LTER plot of Ecohydrology Research Institute. *Chubu Forest Research*, *60*, 147–150 (in Japanese).
- Sawada, H., Hirao, T., & Kamata, N. (2014). Annual increase of infestation by *Platypus quercivorus* (Murayama) and its spatial distribution in a secondary warm-temperate forest stand in Tokai District. *Forest Pests*, *62*, 10–15 (in Japanese).
- Shinozaki, K., Yoda, K., Hozumi, K., & Kira, T. (1964). A quantitative analysis of plant form—the pipe model theory: I. Basic analyses. *Japanese Journal of Ecology*, *14*, 97–132.
- Taneda, H., & Sperry, J. S. (2008). A case-study of water transport in co-occurring ring- versus diffuse-porous trees: Contrasts in water-status, conducting capacity, cavitation and vessel refilling. *Tree Physiology*, *28*, 1641–1651.
- Tyree MT, Ewers FW. 1991. The hydraulic architecture of trees and other woody plants. *New Phytologist* *119*: 345–360. doi:10.1111/j.1469-8137.1991.tb00035.x
- Tyree, M. T., & Sperry, J. S. (1988). Do woody plants operate near the point of catastrophic xylem dysfunction caused by dynamic water stress? *Plant Physiology*, *88*, 0574–0580.
- Urano, T. (2000). Relationships between mass mortality of two oak species (*Quercus mongolica* Turcz. var. *grosseserrata* Rehd. et Wils. and *Q. serrata* Thunb.) and infestation by and reproduction of *Platypus quercivorus* (Murayama) (Coleoptera: Platypodidae). *Journal of Forest Research*, *5*, 187–193.
- Waisel, Y., Lipshitz, N., & Kuller, Z. (1972). Pattern of water movement in trees and shrubs. *Ecology*, *53*, 520–523.
- Wang, Y., Liu, G., Kume, T., Otsuki, K., Yamanaka, N., & Du, S. (2010). Estimating water use of a black locust plantation by the thermal dissipation probe method in the semiarid region of Loess Plateau, China. *Journal of Forest Research*, *15*, 241–251. doi:10.1007/s10310-010-0184-y
- Wilson, K. B., Hanson, P. J., Mulholland, P. J., Baldocchi, D. D., & Wullschlegel, S. D. (2001). A comparison of methods for determining forest evapotranspiration and its components: Sap-flow, soil water budget, eddy covariance and catchment water balance. *Agricultural and Forest Meteorology*, *106*, 153–168.
- Wullschlegel, S. D., & Norby, R. J. (2001). Sap velocity and canopy transpiration in a sweetgum stand exposed to free-air CO<sub>2</sub> enrichment (FACE). *New Phytologist*, *150*, 489–498.
- Yamasaki, M., Ito, Y., & Ando, M. (2014). Mass attack by the ambrosia beetle *Platypus quercivorus* occurs in single trees and in groups of trees. *Canadian Journal of Forest Research*, *44*, 243–249. doi:10.1139/cjfr-2013-0273

## SUPPORTING INFORMATION

Additional Supporting Information may be found online in the supporting information tab for this article.

**How to cite this article:** Chandrathilake, G. G. T., Tanaka, N., and Kamata, N. (2016), Whole-tree sap flux in *Quercus serrata* trees after three levels of partial sapwood removal to simulate Japanese oak wilt, *Ecohydrology*, doi: 10.1002/eco.1797